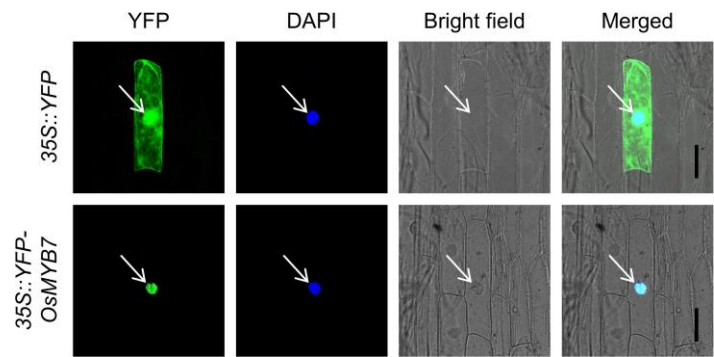


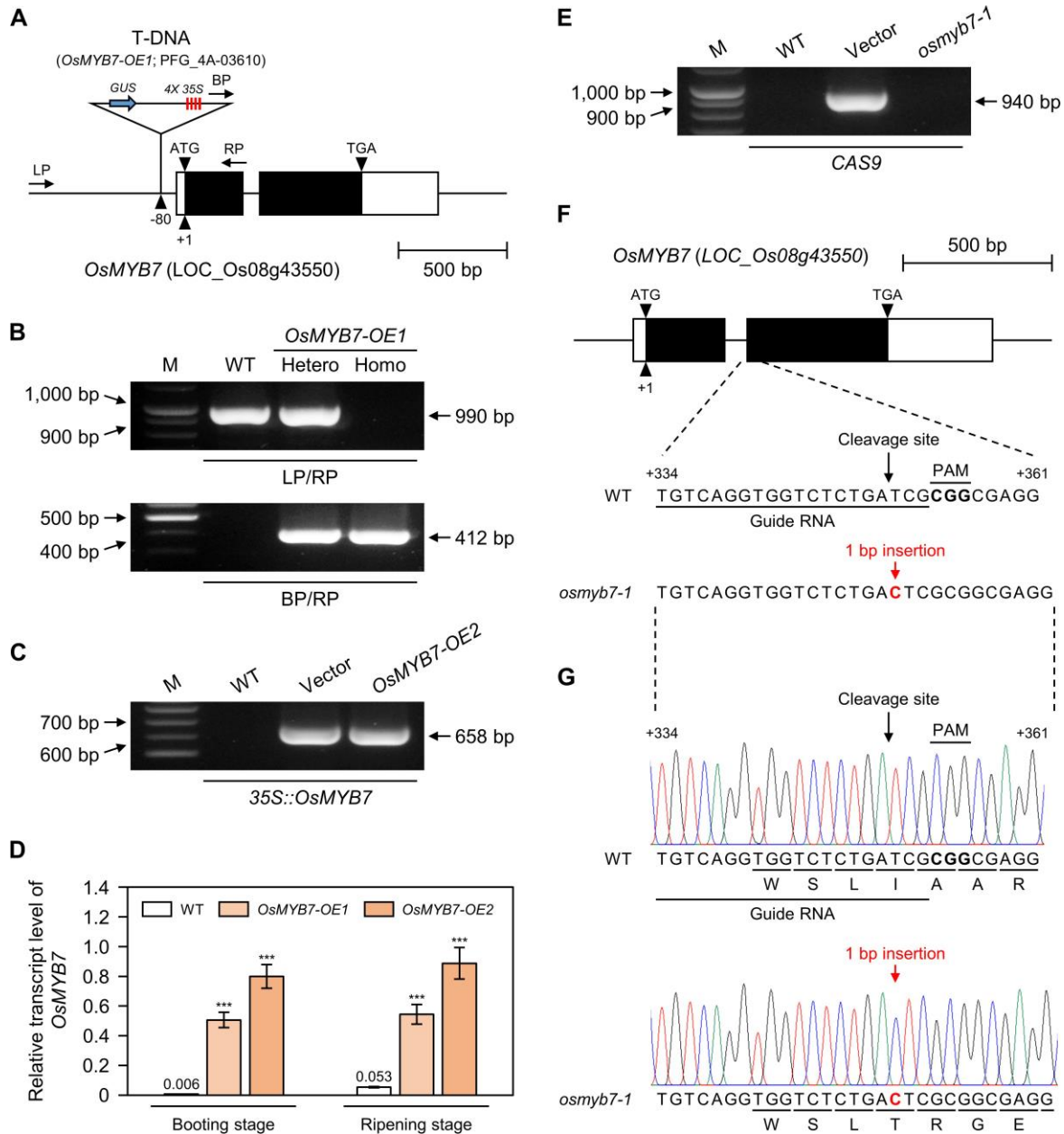
Supplementary materials - Kim et al.

R2 repeat of MYB DNA-binding domain		
OsMYB7	1	MGRSPCCEKEHTNKGAWTKEEDERLVAYIRAHGEGCWRSLPKAAGLLRCGKSCRLRWINY
OsMYB108	1	MGRSPCCEKAHTNKGAWTKEEDDRLIAYIKAHGEGCWRSLPKAAGLLRCGKSCRLRWINY
ZmMYB42	1	MGRSPCCEKAHTNIGAWTKEEDERLVAYIRAHGEGCWRSLPKAAGLLRCGKSCRLRWINY
ZmMYB31	1	MGRSPCCEKAHTNKGAWTKEEDERLVAYIRAHGEGCWRSLPKAAGLLRCGKSCRLRWINY
AtMYB4	1	MGRSPCCEKAHTNKGAWTKEEDERLVAYIRAHGEGCWRSLPKAAGLLRCGKSCRLRWINY
AtMYB7	1	MGRSPCCEKEHMNKGAWTKEEDERLVSYIKSHGEGCWRSLPKAAGLLRCGKSCRLRWINY
AtMYB32	1	MGRSPCCEKDHTNKGAWTKEEDDKLISYIKAHGEGCWRSLPKAAGLLRCGKSCRLRWINY
R3 repeat of MYB DNA-binding domain		
OsMYB7	61	LRPDLKRGNFTADEDILIIKLHSLLGNKWSLIAARLPGRTDNEIKNYWNTHIRRKLLRG
OsMYB108	61	LRPDLKRGNFTEEEDELIELIILKHSSLLGNKWSLIAAGRIPGRTDNEIKNYWNTHIRRKLLSRG
ZmMYB42	61	LRPDLKRGNFTADEDILIVKLHSLLGNKWSLIAARLPGRTDNEIKNYWNTHIRRKLLGSG
ZmMYB31	61	LRPDLKRGNFTEEEDELIVKLHSVLGNKWSLIAAGRIPGRTDNEIKNYWNTHIRRKLLSRG
AtMYB4	61	LRPDLKRGNFTEEEDELIELIILKHSSLLGNKWSLIAAGRIPGRTDNEIKNYWNTHIRRKLINRG
AtMYB7	61	LRPDLKRGNFTHDEDELIELIILKHSSLLGNKWSLIAARLPGRTDNEIKNYWNTHIRRKLINRG
AtMYB32	61	LRPDLKRGNFTLEEDILIIKLHSLLGNKWSLIAARLPGRTDNEIKNYWNTHIRRKLINRG
OsMYB7	121	IDPVTHRPNAA-AATISFHPQPPPTT-----
OsMYB108	121	IDPVTHRPIND-SASNIITISFEAAAA--AARDDKAAVIRREDH-PHQPKAVTV-----
ZmMYB42	121	IDPVTHRVRAGGAATTISFQPSPNSAAAAAAAETAAQA-----
ZmMYB31	121	IDPVTHRVPTEHHASITISFETEVAAAARRDDKGAVIRLEEE-EERNKATMVVGRDRQS
AtMYB4	121	IDPTSHRPIQESSASODSKPTQLEPVTNTIN--ISPTSAPKVFHESISFPCKSE--
AtMYB7	121	IDPATHRGINEAKIS---DLKKTKDQIVKD---VSE---VTKFEETDKSGDQKQN
AtMYB32	121	IDPATHRPINETKTSODSSSSKTEDPLVKI---LSF---GPQLEKIANFGDERIQ
EAR motif		
OsMYB7	147	-----KEEQLILSPPKCPDLNLDLCISPPSCQEEDD-----DYEAKPAMIVRAPE-
OsMYB108	171	---QEQQAAADWGHG-KPLKCPDLNLDLCISLPSQEEPMMM-----
ZmMYB42	159	-----PIKAEETAALKAPRCPDLNLDLCISPPCQHEDDGEDEEELDLKPAFKVREALQ
ZmMYB31	180	QSQSHSHPAGEWGQCKRPLKCPDLNLDLCISPPCQEEEMEEAA-----MRVR---
AtMYB4	176	-KISMLTFKEEKDECPCVQEKFDPDLNLERLRISSLPPDDVDRLO-----
AtMYB7	167	KYIRNGLVCKEERVVVEEKIGPDLNLERLRISSPPWQNQR-----
AtMYB32	171	KRVE-----YSVVEERCLLDLNLERLRISSPPWQDKLHDERN-----
OsMYB7	193	-LQRRGGLCFGCSLGQKECKCSCGGGAGA-----GACNNFLGLR-----
OsMYB108	208	KPVRETGVCFSCSLGLPKSTDCKC-----S-SFLGLR-----
ZmMYB42	213	A GHGHGHGLCLGCGLGGQKGA---AGCSC-----SNCHHFLGLR-----
ZmMYB31	228	PAVREAGLCFGCSLGIPRTADCCKC-----SSSSFLGLR-----
AtMYB4	215	GHGKSTTPRCEFKCSLGMINGMECRGGRMRCDVVGSSKG-----SDMSNCFDFLGLAKK
AtMYB7	205	----EISTCTASRFYENDMECSSETVKCQTENSSSIYSSSIDISSNVCYDFLGLK-----
AtMYB32	205	LRFGRVKYRCSCAGCFGNGKECSNNVKCQTEDSSSSYSTDISS-SICYDFLGLN-----
OsMYB7	232	--AGILDFRSLPMK
OsMYB108	240	--TAMLDFRSLEMK
ZmMYB42	249	--TSVLDFRGLEMK
ZmMYB31	262	--TAMLDFRSLEMK
AtMYB4	269	ETTSILGFRSLEMK
AtMYB7	258	--TRILDFRSLEMK
AtMYB32	262	-NTRVLDGSTLEMK

SUPPLEMENTARY FIGURE S1. Multiple sequence alignment of OsMYB7 homologs in *Oryza sativa*, *Zea mays*, and *Arabidopsis thaliana*. The amino acid sequences of OsMYB7 homologs acquired from the National Center for Biotechnology Information website (<https://www.ncbi.nlm.nih.gov/>) were subjected to protein sequence alignment using Clustal Omega from the EMBL-EBI website (<https://www.ebi.ac.uk/Tools/msa/clustalo/>) and the BoxShade 3.21 server (<http://arete.ibb.waw.pl/PL/html/boxshade.html>). Homologous regions are highlighted in black for identical amino acid residues or in gray for conservative amino acid substitutions. OsMYB108, ZmMYB42, ZmMYB31, AtMYB4, AtMYB7, and AtMYB32 show 65.9%, 66.2%, 60.8%, 55.7%, 54.7%, and 52.5% sequence similarity to OsMYB7, respectively, according to the NCBI-BLASTP program (https://blast.ncbi.nlm.nih.gov/Blast.cgi?PROGRAM=blastp&PAGE_TYPE=BlastSearch&LINK_LOC=blasthome). The conserved regions, such as R2 and R3 repeats of the MYB DNA-binding domain, and the EAR motif, are indicated by black lines. Numbers to the left side of each sequence represent amino acid positions. GenBank accession numbers of protein sequences are as follows: OsMYB7, XP_015650911; OsMYB108, XP_015612022; ZmMYB42, ADX60106; ZmMYB31, NP_001105949; AtMYB4, NP_195574; AtMYB7, NP_179263; AtMYB32, NP_195225. EAR, ethylene-responsive element binding factor-associated amphiphilic repression.

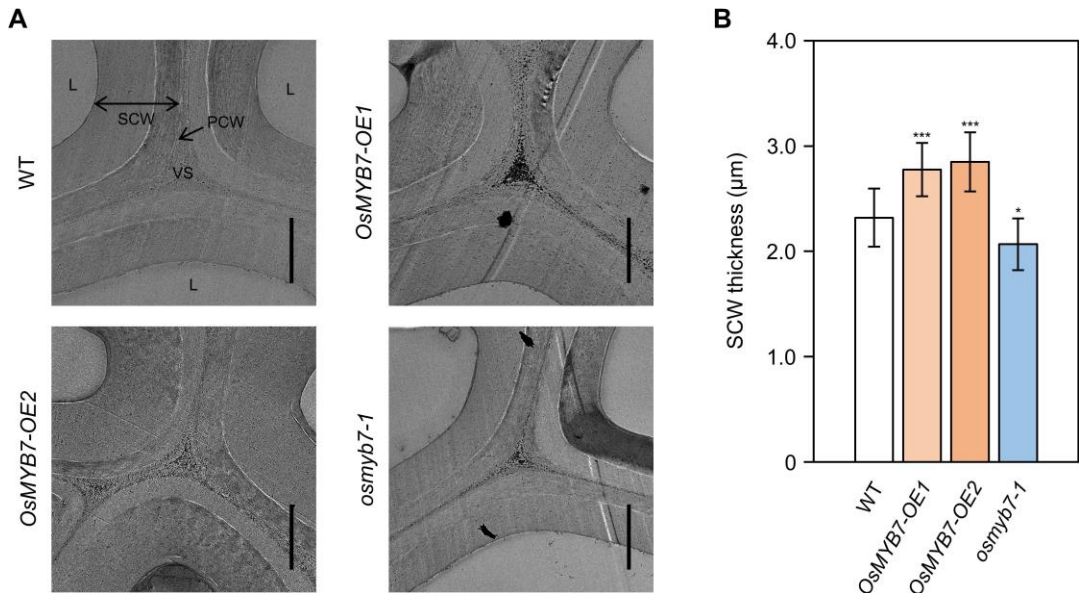


SUPPLEMENTARY FIGURE S2. Subcellular localization of OsMYB7. DAPI-stained onion epidermal cells expressing YFP-OsMYB7 were observed using a confocal laser scanning microscope. Cells expressing YFP were used as a control. The white arrows point to the nucleus of each cell. Scale: 100 μ m. Data shown are representatives of three independent experiments. DAPI, 4',6-diamidino-2-phenylindole; YFP, yellow fluorescent protein.

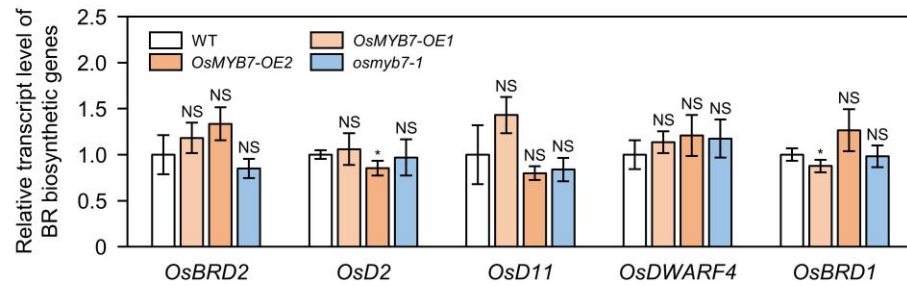
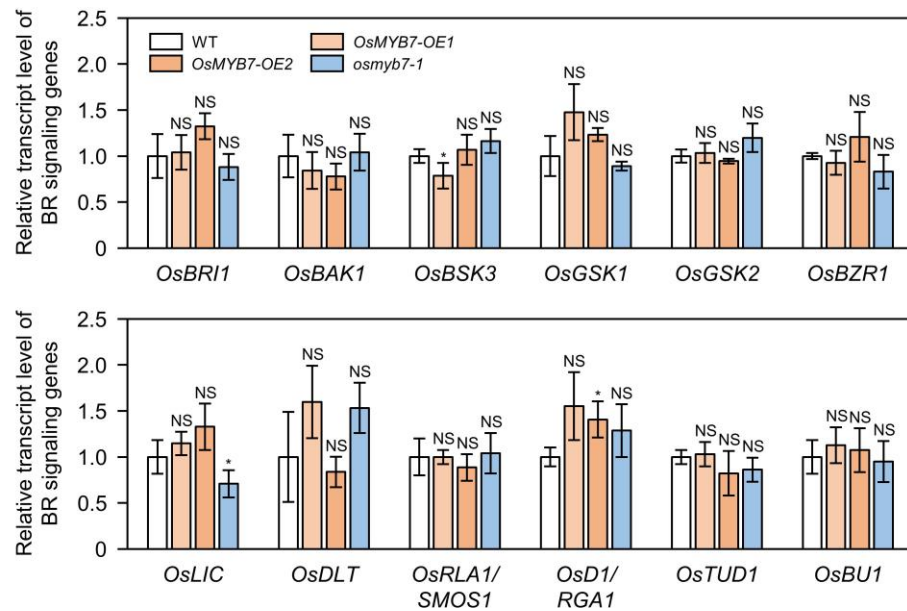


SUPPLEMENTARY FIGURE S3. Information of plant materials used in this study. **(A)** Schematic diagram illustrating the position of the T-DNA insertion in OsMYB7-OE1. Open and filled boxes indicate untranslated regions and exons, respectively. The position of the T-DNA insertion is shown relative to that of the translation initiation codon, which was set as +1. The promoterless *GUS* reporter gene and multimerized CaMV 35S enhancer harbored by the T-DNA are shown as the blue solid arrow and red vertical lines, respectively. Blac

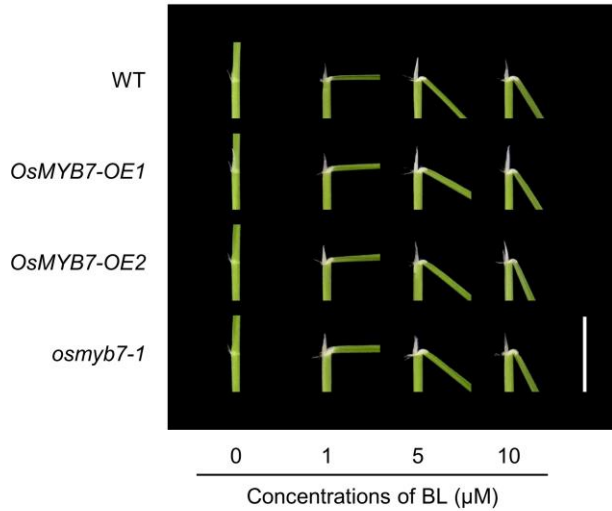
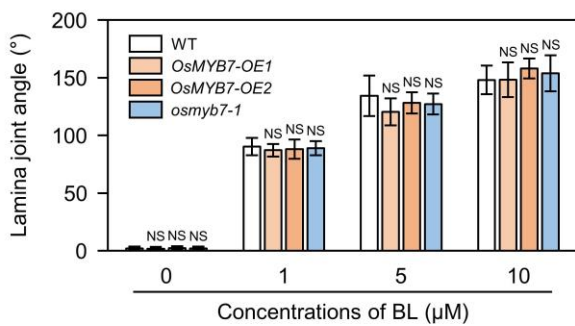
k arrows indicate the primers used for PCR genotyping. BP, border primer; 4X 35S, tetramerized CaMV 35S enhancer; *GUS*, β -glucuronidase; LP, left primer; RP, right primer. **(B)** Identification of the T-DNA insertion in *OsMYB7-OE1*. Genomic DNA from the T_2 segregating population was isolated from individual plants and subjected to PCR using the primers denoted in **(A)**. LP + RP primers amplify the 990-bp WT allele; BP + RP primers amplify the 412-bp T-DNA fragment. Plants homozygous for the T-DNA insertion were selected and used for further study. M, marker. **(C)** Confirmation of rice transformation in *OsMYB7-OE2* by genomic PCR. The 35S:*OsMYB7* construct was introduced into rice callus to generate *OsMYB7-OE2*. Genomic DNA of the resulting T_0 plants was extracted, followed by PCR analysis using a primer set that amplifies part of the 35S:*OsMYB7* construct. WT and the 35S:*OsMYB7* construct were used as a negative and positive control, respectively. M, marker. **(D)** Relative *OsMYB7* transcript levels in WT, *OsMYB7-OE1*, and *OsMYB7-OE2* plants. Total RNA isolated from flag leaf lamina joints of plants at the booting stage (105 DAS) or at the ripening stage (30 DAH) grown in a natural paddy field was subjected to RT-qPCR analysis, with *GAPDH* serving as a reference for normalization. Data are presented as means \pm SD ($n = 4$). Asterisks indicate significant differences compared to WT as determined by two-tailed Student's *t*-test (** $P < 0.001$). DAH, days after heading; DAS, days after sowing. **(E)** PCR verification of the T-DNA free *osmyb7-1* mutant. The T-DNA encoding both Cas9 protein and *OsMYB7*-targeted single guide RNA was introduced into rice callus to generate *osmyb7-1*. Genomic DNA was isolated for the resulting T_1 segregating population and subjected to PCR analysis using a primer set that amplifies part of Cas9 to obtain transgene-free *osmyb7-1* mutant plants for further study. WT and the vector containing Cas9 were used as a negative and positive control, respectively. M, marker. **(F)** Schematic diagram showing the position of the target site for *OsMYB7* gene editing described in **(E)**. The 20-nt spacer region in *OsMYB7* is underlined, and the PAM is emphasized in bold. The location of the Cas9 cleavage site, 3-4 bp upstream of the PAM, is shown as a black arrow. Nucleotide numbering is relative to the ATG start codon. PAM, protospacer adjacent motif. **(G)** Chromatograms of direct sequencing results from genomic PCR products of WT and the *osmyb7-1* mutant. The *OsMYB7* genomic DNA region around the target site illustrated in **(F)** was amplified, and the resulting PCR products were subjected to direct Sanger sequencing.



SUPPLEMENTARY FIGURE S4. Transmission electron microscopic analysis of the lamina joint. **(A)** Secondary cell walls of sclerenchyma cells at lamina joints. Collars of flag leaves from WT, *OsMYB7-OE1*, *OsMYB7-OE2*, and *osmyb7-1* plants at the ripening stage (30 DAH) grown under natural day-night conditions were sampled for examination. Scale: 2 μ m. Images shown are representatives of four independent experiments. L, lumen; PCW, primary cell wall; SCW, secondary cell wall; VS, void space. **(B)** Quantitative data of the secondary cell wall thickness in **(A)**. Data are presented as means \pm SD from at least ten cells. Asterisks denote significant differences, as determined by two-tailed Student's *t*-test (* $P < 0.05$ and *** $P < 0.001$).

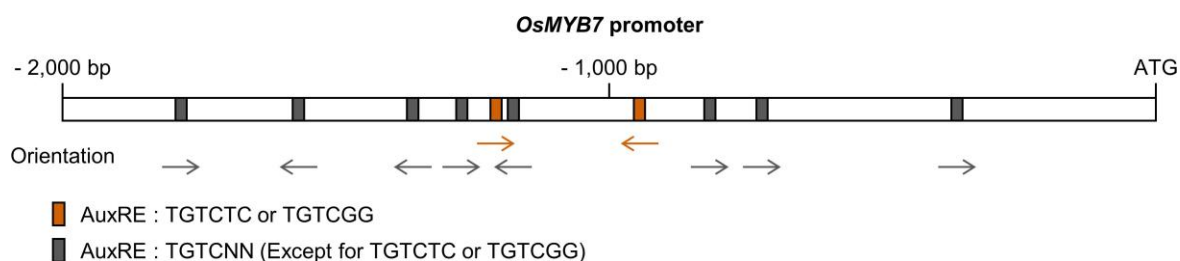
A**B**

SUPPLEMENTARY FIGURE S5. Transcript levels of representative BR-related genes that regulate leaf inclination. **(A, B)** Relative expression levels of BR biosynthetic **(A)** and signaling **(B)** genes in WT, OsMYB7-OE1, OsMYB7-OE2, and osmyb7-1 plants. Samples harvested in **Figure 4A** were subjected to RT-qPCR analysis, using *GAPDH* as an internal control. The normalized transcript levels of each gene are presented relative to those in WT, which were set to 1. Data are presented as means \pm SD of four biological replicates. Asterisks indicate significant differences compared to WT as determined by two-tailed Student's *t*-test; * $P < 0.05$. These experiments were repeated twice with similar results. NS, not significant.

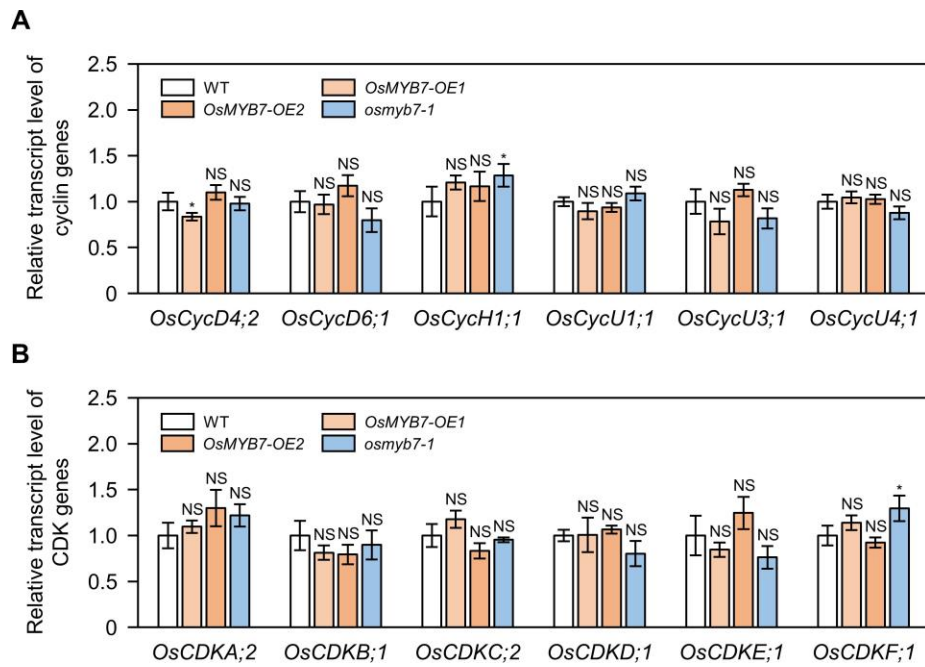
A**B**

SUPPLEMENTARY FIGURE S6. BR-induced lamina joint inclination assay. **(A)** Effects of BL on the lamina inclination of WT, OsMYB7-OE1, OsMYB7-OE2, and *osmyb7-1*. Plants were grown in paddy soil for 10 days under long-day conditions (14.5 h light, 30°C / 9.5 h dark, 24°C) with 60% relative humidity in an artificial growth chamber. Approximately 2-cm of lamina joint segments, consisting of leaf blade, lamina joint at S4 developmental stage, and leaf sheath, were excised from uniform seedlings, followed by incubation in distilled water containing 0, 1, 5, or 10 μM of BL under dark conditions at 30°C for 48 h. The excised segments were kept in a vertical orientation to minimize gravitropic response of the lamina joint. Photographs of representative lamina joint segments for each group were taken. Scale: 1 cm. **(B)** Lamina joint angle shown in **(A)**. Degrees of the leaf blade angle against the axis of leaf sheath were measured with a protractor. Data are presented as means \pm SD from ten lamina joint segments. Statistical analysis using two-tailed Student's *t*-test revealed no obvious differences in lamina inclination of OsMYB7-OE1, OsMYB7-

OE2, and *osmyb7-1* segments compared to that of WT segments. These experiments were performed twice yielding similar results. BL, 24-epibrassinolide; NS, not significant.



SUPPLEMENTARY FIGURE S7. Identification of putative AuxREs in the promoter of *OsMYB7*. Sequence of the *OsMYB7* promoter (-2,000 bp to -1 bp from the initiation codon) obtained from the Gramene website (<https://www.gramene.org/>) is shown as a schematic diagram. Positions and orientations of the AuxREs, TGTCNN consensus core sequences, are presented as filled boxes and arrows, respectively, in gray. The canonical AuxREs, such as TGTCTC and TGTCGG, are highlighted in yellow red. AuxRE, auxin-responsive element.



SUPPLEMENTARY FIGURE S8. Expression profiles of cell division-related genes at lamina joints of WT, OsMYB7-OE1, OsMYB7-OE2, and *osmyb7-1* plants. **(A, B)** Relative transcript levels of cyclin (**A**) and CDK (**B**) genes. The cDNA samples in **Figure 4A** were subjected to RT-qPCR analysis, with *GAPDH* used as reference for normalization, and shown relative to those in WT, which were set to 1. Data are presented as means \pm SD from four independent biological replicates. Asterisks indicate significant differences as determined by two-tailed Student's *t*-test (* $P < 0.05$). These experiments were performed twice yielding similar results. CDK, cyclin-dependent kinase; NS, not significant.

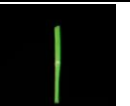
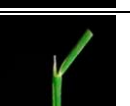
SUPPLEMENTARY TABLE S1. *In silico* analysis for subcellular localization of OsMYB7 homologs.

	Plastid	Cytoplasm	Extra-cellular	Nucleus	Mito-chondrion	Cell Membrane	Endo-plasmic Reticulum
OsMYB7	0.0745 (7.4%)	0.229 (23%)	0.00249 (0.25%)	0.431 (43%)	0.0736 (7.4%)	0.0523 (5.2%)	0.015 (1.5%)
OsMYB108	0.00797 (0.80%)	0.0159 (1.6%)	0.00032 (0.032%)	0.864 (86%)	0.00485 (0.48%)	0.0414 (4.1%)	0.0092 (0.92%)
ZmMYB42	0.0349 (3.5%)	0.0256 (2.6%)	0.00122 (0.12%)	0.684 (68%)	0.0128 (1.3%)	0.147 (15%)	0.0105 (1.0%)
ZmMYB31	0.00562 (0.56%)	0.0232 (2.3%)	0.000544 (0.054%)	0.799 (80%)	0.00551 (0.55%)	0.0367 (3.7%)	0.0166 (1.7%)
AtMYB4	0.0424 (4.2%)	0.0847 (8.5%)	0.000841 (0.084%)	0.729 (73%)	0.016 (1.6%)	0.0324 (3.2%)	0.00888 (0.89%)
AtMYB7	0.0279 (2.8%)	0.0457 (4.6%)	0.000357 (0.036%)	0.716 (72%)	0.00311 (0.31%)	0.0365 (3.6%)	0.0217 (2.2%)
AtMYB32	0.0206 (2.1%)	0.0316 (3.2%)	0.000219 (0.022%)	0.822 (82%)	0.00181 (0.18%)	0.0139 (1.4%)	0.0141 (1.4%)

	Golgi Apparatus	Vacuole	Peroxisome	Cell Wall	Mito-chondrion / Plastid	Cytoplasm / Nucleus	Cytoplasm / Golgi Apparatus
OsMYB7	0.0194 (1.9%)	0.00741 (0.74%)	0.0229 (2.3%)	0.00237 (0.24%)	0.00586 (0.59%)	0.0606 (6.1%)	0.00348 (0.35%)
OsMYB108	0.00867 (0.87%)	0.00102 (0.10%)	0.0103 (1.0%)	0.00037 (0.037%)	0.00137 (0.14%)	0.0332 (3.3%)	0.00107 (0.11%)
ZmMYB42	0.0243 (2.4%)	0.00477 (0.48%)	0.013 (1.3%)	0.000641 (0.064%)	0.00563 (0.56%)	0.0336 (3.4%)	0.00197 (0.20%)
ZmMYB31	0.00848 (0.85%)	0.00156 (0.16%)	0.00918 (0.92%)	0.000563 (0.056%)	0.00225 (0.22%)	0.0898 (9.0%)	0.000912 (0.091%)
AtMYB4	0.00912 (0.91%)	0.00198 (0.20%)	0.0101 (1.0%)	0.000784 (0.078%)	0.00229 (0.23%)	0.0605 (6.0%)	0.00115 (0.12%)
AtMYB7	0.00352 (0.35%)	0.0026 (0.26%)	0.00395 (0.40%)	0.000663 (0.066%)	0.000577 (0.058%)	0.137 (14%)	0.000889 (0.089%)
AtMYB32	0.0086 (0.86%)	0.000875 (0.088%)	0.00366 (0.37%)	0.000235 (0.024%)	0.000246 (0.025%)	0.0812 (8.1%)	0.000655 (0.066%)

The protein sequences of OsMYB7 homologs in **Supplementary Figure S1** were analyzed using the PseAAC-NCC-DIPEP prediction module of Plant-mSubP program (<http://bioinfo.usu.edu/Plant-mSubP/>), one of the *in silico* analysis tools for subcellular localization of proteins in plant cell. Values in the table represent likelihoods of localization to the corresponding organelles. All the OsMYB7 homologs were predicted to be nuclear proteins with the highest localization likelihoods, and the values of nucleus for each protein were highlighted in red letters.

SUPPLEMENTARY TABLE S2. Six developmental stages of the lamina joint.

Stage	Morphological features	Representative image	Reference
S1 (Initiation)	> Lamina joint differentiation is initiated > Lamina joint is transparent and hollow		Zhou, L. J., Xiao, L. T., Xue, H. W. (2017). Dynamic cytology and transcriptional regulation of rice lamina joint development. <i>Plant Physiol.</i> 174, 1728-1746. doi: 10.1104/pp.17.00413
S2 (Young)	> Lamina joint protrudes and becomes larger > Lamina joint is white or creamy yellow		
S3 (Young)	> Lamina joint is still enclosed by leaf sheath > A ligule and a pair of auricles can be observed		
S4 (Maturation)	> Lamina joint emerges from leaf sheath > Leaf blade and leaf sheath fully developed		
S5 (Post-maturation)	> Asymmetric cell elongation and/or division between the abaxial and adaxial sides lead to increased leaf angle		
S6 (Senescence)	> Lamina joint reaches the maximum angle > Lamina joint begins to wither due to water loss		

SUPPLEMENTARY TABLE S3. Genes described in this study and their corresponding locus IDs.

A. OsMYB7 and GAPDH				
Gene	MSU_Locus	RAP_Locus	Accession No.	Reference
<i>OsMYB7</i>	LOC_Os08g43550	Os08g0549000	CI473176	Miyamoto et al., 2019
<i>GAPDH</i>	LOC_Os04g40950	Os04g0486600	AK064960	Jain et al., 2006
B. OsbHLH079 and ONAC026				
Gene	MSU_Locus	RAP_Locus	Accession No.	Reference
<i>OsbHLH079</i>	LOC_Os02g47660	Os02g0705500	AK119183	Seo et al., 2020
<i>ONAC026</i>	LOC_Os01g29840	Os01g0393100	AK107407	Mathew et al., 2016
C. Lignin biosynthetic genes				
Gene	MSU_Locus	RAP_Locus	Accession No.	Reference
<i>OsPAL1</i>	LOC_Os02g41630	Os02g0626100	AK060724	Tonnessen et al., 2015
<i>OsPAL2</i>	LOC_Os02g41650	Os02g0626400	AK060724	
<i>OsC4H2</i>	LOC_Os05g25640	Os05g0320700	AK104994	Yang et al., 2005
<i>Os4CL3</i>	LOC_Os02g08100	Os02g0177600	AK070083	Gui et al., 2011
<i>OsHCT1</i>	LOC_Os04g42250	Os04g0500700	AK072528	
<i>OsHCT2</i>	LOC_Os02g39850	Os02g0611800	AK104319	Kim et al., 2012
<i>OsC3H</i>	LOC_Os05g41440	Os05g0494000	AK099695	Takeda et al., 2018
<i>OsCOA1</i>	LOC_Os06g06980	Os06g0165800	AK065744	
<i>OsCOA20</i>	LOC_Os08g38900	Os08g0498100	AK104326	Zhao et al., 2004
<i>OsCCoAOMT1</i>	LOC_Os08g38910	Os08g0498400	AK061757	
<i>OsCOMT1</i>	LOC_Os08g06100	Os08g0157500	AK064768	
<i>OsCCR17</i>	LOC_Os09g04050	Os09g0127300	AK100234	
<i>OsCCR19</i>	LOC_Os09g25150	Os09g0419200	AK104860	
<i>OsCCR20</i>	LOC_Os08g34280	Os08g0441500	AK072872	
<i>OsCAD2</i>	LOC_Os02g09490	Os02g0187800	AK105011	
<i>OsCAD6</i>	LOC_Os04g15920	Os04g0229100	AK099270	Park et al., 2018
D. Cellulose biosynthetic genes				
Gene	MSU_Locus	RAP_Locus	Accession No.	Reference
<i>OsCESA1</i>	LOC_Os05g08370	Os05g0176100	AK099281	
<i>OsCESA3</i>	LOC_Os07g24190	Os07g0424400	AK120236	
<i>OsCESA5</i>	LOC_Os03g62090	Os03g0837100	AK100877	
<i>OsCESA6</i>	LOC_Os07g14850	Os07g0252400	AK100914	
<i>OsCESA8</i>	LOC_Os07g10770	Os07g0208500	AK072356	
<i>OsCSLA1</i>	LOC_Os02g09930	Os02g0192500	AK059580	
<i>OsCSLA6</i>	LOC_Os02g51060	Os02g0744600	AK058756	
<i>OsCSLC1</i>	LOC_Os01g56130	Os01g0766900	AK110759	
<i>OsCSLC7</i>	LOC_Os05g43530	Os05g0510800	AF435642	
<i>OsCSLC9</i>	LOC_Os03g56060	Os03g0770800	AK121805	
<i>OsCSLD2</i>	LOC_Os06g02180	Os06g0111800	AK105393	
<i>OsCSLE1</i>	LOC_Os09g30120	Os09g0478100	AK102766	
<i>OsCSLF6</i>	LOC_Os08g06380	Os08g0160500	AK109812	
<i>OsCSLH1</i>	LOC_Os10g20090	Os10g0341700	AK121003	
E. Brassinosteroid (BR) biosynthetic genes				
Gene	MSU_Locus	RAP_Locus	Accession No.	Reference
<i>OsBRD2</i>	LOC_Os10g25780	Os10g0397400	AK111949	
<i>OsD2</i>	LOC_Os01g10040	Os01g0197100	C97895	
<i>OsD11</i>	LOC_Os04g39430	Os04g0469800	AK106528	
<i>OsDWARF4</i>	LOC_Os03g12660	Os03g0227700	CI552150	
<i>OsBRD1</i>	LOC_Os03g40540	Os03g0602300	AK072295	
F. Brassinosteroid (BR) signaling genes				
Gene	MSU_Locus	RAP_Locus	Accession No.	Reference
<i>OsBRI1</i>	LOC_Os01g52050	Os01g0718300	AK101085	
<i>OsBAK1</i>	LOC_Os08g07760	Os08g0174700	AK103038	
<i>OsBSK3</i>	LOC_Os04g58750	Os04g0684200	AK101506	
<i>OsGSK1</i>	LOC_Os01g10840	Os01g0205700	AK099863	
<i>OsGSK2</i>	LOC_Os05g11730	Os05g0207500	AK102147	
<i>OsBZR1</i>	LOC_Os07g39220	Os07g0580500	AK106748	
<i>OsLIC</i>	LOC_Os06g49080	Os06g0704300	AK107008	Xu et al., 2021

<i>OsDLT</i>	LOC_Os06g03710	Os06g0127800	AK106449	
<i>OsRLA1/SMOS1</i>	LOC_Os05g32270	Os05g0389000	AK059324	
<i>OsD1/RGA1</i>	LOC_Os05g26890	Os05g0333200	D38232	
<i>OsTUD1</i>	LOC_Os03g13010	Os03g0232600	AK068218	
<i>OsBU1</i>	LOC_Os06g12210	Os06g0226500	AK071601	
G. Auxin biosynthetic genes				
Gene	MSU_Locus	RAP_Locus	Accession No.	Reference
<i>OsTAA1</i>	LOC_Os01g07500	Os01g0169800	AK061054	Yoshikawa et al., 2014
<i>OsYUCCA3</i>	LOC_Os01g53200	Os01g0732700	AP014957	Zhang et al., 2018
<i>OsYUCCA4</i>	LOC_Os01g12490	Os01g0224700	AK070386	
<i>OsYUCCA5</i>	LOC_Os12g32750	Os12g0512000	C98496	
<i>OsYUCCA6</i>	LOC_Os07g25540	Os07g0437000	CI249850	
<i>OsYUCCA7</i>	LOC_Os04g03980	Os04g0128900	AK068976	
H. Auxin conjugation genes				
Gene	MSU_Locus	RAP_Locus	Accession No.	Reference
<i>OsGH3-1</i>	LOC_Os01g57610	Os01g0785400	AK063368	Terol et al., 2006
<i>OsGH3-3</i>	LOC_Os01g12160	Os01g0221100	AK072125	
<i>OsGH3-4</i>	LOC_Os05g42150	Os05g0500900	AK101932	
<i>OsGH3-6</i>	LOC_Os05g05180	Os05g0143800	AK106538	
<i>OsGH3-7</i>	LOC_Os06g30440	Os06g0499500	AK107353	
<i>OsDAO</i>	LOC_Os04g39980	Os04g0475600	AK105400	Zhao et al., 2013
I. Cyclin genes				
Gene	MSU_Locus	RAP_Locus	Accession No.	Reference
<i>OsCycD4;2</i>	LOC_Os08g37390	Os08g0479300	AK070025	La et al., 2006
<i>OsCycD6;1</i>	LOC_Os07g37010	Os07g0556000	AK121938	
<i>OsCycH1;1</i>	LOC_Os03g52750	Os03g0737600	AK101854	
<i>OsCycU1;1</i>	LOC_Os04g53680	Os04g0628900	AP014960	
<i>OsCycU3;1</i>	LOC_Os05g33040	Os05g0398000	AK070478	
<i>OsCycU4;1</i>	LOC_Os10g41430	Os10g0563900	AK107529	
J. Cyclin-dependent kinase (CDK) genes				
Gene	MSU_Locus	RAP_Locus	Accession No.	Reference
<i>OsCDKA;2</i>	LOC_Os02g03060	Os02g0123100	AK101344	Guo et al., 2007
<i>OsCDKB;1</i>	LOC_Os01g67160	Os01g0897000	C1522617	
<i>OsCDKC;2</i>	LOC_Os01g72790	Os01g0958000	AK103469	
<i>OsCDKD;1</i>	LOC_Os05g32600	Os05g0392300	AK120162	
<i>OsCDKE;1</i>	LOC_Os10g42950	Os10g0580300	AK066824	
<i>OsCDKF;1</i>	LOC_Os06g22820	Os06g0334400	AK059487	
K. Expansin genes				
Gene	MSU_Locus	RAP_Locus	Accession No.	Reference
<i>OsEXPB1</i>	LOC_Os04g15840	Os04g0228400	AK069548	Sampedro et al., 2005
<i>OsEXPB4</i>	LOC_Os05g39990	Os05g0477600	AK100179	
<i>OsEXPB6</i>	LOC_Os03g21820	Os03g0336400	AK107698	
<i>OsEXPB10</i>	LOC_Os04g49410	Os04g0583500	AK066414	
<i>OsEXPB3</i>	LOC_Os10g40720	Os10g0555900	AK100959	
<i>OsEXPB4</i>	LOC_Os10g40730	Os10g0556100	AK060096	
<i>OsEXPB6</i>	LOC_Os10g40700	Os10g0555600	AK105799	
<i>OsEXLA2</i>	LOC_Os10g39640	Os10g0542400	AK068088	
<i>OsEXLA3</i>	LOC_Os07g29290	Os07g0475400	AK102489	
L. Xyloglucan endotransglucosylase/hydrolase (XTH) genes				
Gene	MSU_Locus	RAP_Locus	Accession No.	Reference
<i>OsXTH9</i>	LOC_Os04g51460	Os04g0604300	AF443603	Yokoyama et al., 2004
<i>OsXTH10</i>	LOC_Os06g48200	Os06g0697000	AK105513	
<i>OsXTH11</i>	LOC_Os06g48160	Os06g0696400	AK058291	
<i>OsXTH12</i>	LOC_Os06g48180	Os06g0696600	AK105934	
<i>OsXTH15</i>	LOC_Os06g22919	Os06g0335900	AK120283	
<i>OsXTH17</i>	LOC_Os08g13920	Os08g0237000	AK060654	
<i>OsXTH21</i>	LOC_Os07g29750	Os07g0480800	CI419522	
<i>OsXTH23</i>	LOC_Os02g46910	Os02g0696500	AK111242	
<i>OsXTH28</i>	LOC_Os03g13570	Os03g0239000	AK061284	
M. References				

- Castorina, G., and Consonni, G. (2020). The role of brassinosteroids in controlling plant height in Poaceae: a genetic perspective. *Int. J. Mol. Sci.* 157, 574-586. doi: 10.3390/ijms21041191
- Gui, J., Shen, J., Li, L. (2011). Functional characterization of evolutionarily divergent 4-coumarate:coenzyme A ligases in rice. *Plant Physiol.* 157, 574-586. doi: 10.1104/pp.111.178301
- Guo, J., Song, J., Wang, F., Zhang, X. S. (2007). Genome-wide identification and expression analysis of rice cell cycle genes. *Plant Mol. Biol.* 64, 349-360. doi: 10.1007/s11103-007-9154-y
- Hamberger, B., Ellis, M., Friedmann, M., de Azevedo Souza, C., Barbazuk, B., Douglas, C. J. (2008). Genome-wide analyses of phenylpropanoid-related genes in *Populus trichocarpa*, *Arabidopsis thaliana*, and *Oryza sativa*: the *Populus* lignin toolbox and conservation and diversification of angiosperm gene families. *Botany* 85, 1182-1201. doi: 10.1139/B07-098
- Jain, M., Nijhawan, A., Tyagi, A. K., Khurana, J. P. (2006). Validation of housekeeping genes as internal control for studying gene expression in rice by quantitative real-time PCR. *Biochem. Biophys. Res. Commun.* 345, 646-651. doi: 10.1016/j.bbrc.2006.04.140
- Kim, I. A., Kim, B. G., Kim, M., Ahn, J. H. (2012). Characterization of hydroxycinnamoyltransferase from rice and its application for biological synthesis of hydroxycinnamoyl glycerols. *Phytochemistry* 76, 25-31. doi: 10.1016/j.phytochem.2011.12.015
- La, H., Li, J., Ji, Z., Cheng, Y., Li, X., Jiang, S., et al. (2006). Genome-wide analysis of cyclin family in rice (*Oryza Sativa L.*). *Mol. Genet. Genom.* 275, 374-386. doi: 10.1007/s00438-005-0093-5
- Lee, Y. J., Kim, B. G., Chong, Y., Lim, Y., Ahn, J. H. (2008). Cation dependent O-methyltransferases from rice. *Planta* 227, 641-647. doi: 10.1007/s00425-007-0646-4
- Mathew, I. E., Das, S., Mahto, A., Agarwal, P. (2016). Three rice NAC transcription factors heteromerize and are associated with seed size. *Front Plant Sci.* 7, 1638. doi: 10.3389/fpls.2016.01638
- Miyamoto, T., Takada, R., Tobimatsu, Y., Takeda, Y., Suzuki, S., Yamamura, M., et al. (2019). OsMYB108 loss-of-function enriches p-coumaroylated and tricin lignin units in rice cell walls. *Plant J.* 98, 975-987. doi: 10.1111/tpj.14290
- Park, H. L., Bhoo, S. H., Kwon, M., Lee, S. W., Cho, M. H. (2017). Biochemical and expression analyses of the rice cinnamoyl-CoA reductase gene family. *Front. Plant Sci.* 8, 2099. doi: 10.3389/fpls.2017.02099
- Park, H. L., Kim, T. L., Bhoo, S. H., Lee, T. H., Lee, S. W., Cho, M. H. (2018). Biochemical characterization of the rice cinnamyl alcohol dehydrogenase gene family. *Molecules* 23, 2659. doi: 10.3390/molecules23102659
- Sampedro, J., Lee, Y., Carey, R. E., DePamphilis, C., Cosgrove, D. J. (2005). Use of genomic history to improve phylogeny and understanding of births and deaths in a gene family. *Plant J.* 44, 409-419. doi: 10.1111/j.1365-313X.2005.02540.x
- Seo, H., Kim, S. H., Lee, B. D., Lim, J. H., Lee, S. J., An, G., et al. (2020). The rice basic Helix-Loop-Helix 79 (OsbHLH079) determines leaf angle and grain shape. *Int. J. Mol. Sci.* 21, 2090. doi: 10.3390/ijms21062090
- Takeda, Y., Tobimatsu, Y., Karlen, S. D., Koshiba, T., Suzuki, S., Yamamura, M., et al. (2018). Downregulation of p-COUMAROYL ESTER 3-HYDROXYLASE in rice leads to altered cell wall structures and improves biomass saccharification. *Plant J.* 95, 796-811. doi: 10.1111/tpj.13988
- Terol, J., Domingo, C., Talón, M. (2006). The GH3 family in plants: genome wide analysis in rice and evolutionary history based on EST analysis. *Gene* 371, 279-290. doi: 10.1016/j.gene.2005.12.014
- Tonnessen, B. W., Manosalva, P., Lang, J. M., Baraoian, M., Bordeos, A., Mauleon, R., et al. (2015). Rice phenylalanine ammonia-lyase gene *OsPAL4* is associated with broad spectrum disease resistance. *Plant Mol. Biol.* 87, 273-286. doi: 10.1007/s11103-014-0275-9
- Wang, L., Guo, K., Li, Y., Tu, Y., Hu, H., Wang, B., et al. (2010). Expression profiling and integrative analysis of the CESA/CSL superfamily in rice. *BMC Plant Biol.* 10, 282. doi: 10.1186/1471-2229-10-282
- Xu, J., Wang, J. J., Xue, H. W., Zhang, G. H. (2021). Leaf direction: lamina joint development and environmental responses. *Plant Cell Environ.* 44, 2441-2454. doi: 10.1111/pce.14065
- Yang, D. H., Chung, B. Y., Kim, J. S., Kim, J. H., Yun, P. Y., Lee, Y. K., et al. (2005). cDNA cloning and sequence analysis of the rice Cinnamate-4-Hydroxylase gene, a cytochrome P450-dependent monooxygenase involved in the general phenylpropanoid pathway. *J. Plant Biol.* 48, 311-318. doi: 10.1007/BF03030528
- Yokoyama, R., Rose, J. K. C., Nishitani, K. (2004). A surprising diversity and abundance of xyloglucan endotransglucosylase/hydrolases in rice. Classification and expression analysis. *Plant Physiol.* 134, 1088-1099. doi: 10.1104/pp.103.035261
- Yoshikawa, T., Ito, M., Sumikura, T., Nakayama, A., Nishimura, T., Kitano, H., et al. (2014). The rice *FISH BONE* gene encodes a tryptophan aminotransferase, which affects pleiotropic auxin-related processes. *Plant J.* 78, 927-936. doi: 10.1111/tpj.12517
- Zhang, T., Li, R., Xing, J., Yan, L., Wang, R., Zhao, Y. (2018). The YUCCA-Auxin-WOX11 module controls crown root development in rice. *Front. Plant Sci.* 9, 523. doi: 10.3389/fpls.2018.00523
- Zhao, H., Sheng, Q., Lü, S., Wang, T., Song, Y. (2004). Characterization of three rice CCoAOMT genes. *Chin. Sci. Bull.* 49, 1602-1606. doi: 10.1007/BF03184129
- Zhao, Z., Zhang, Y., Liu, X., Zhang, X., Liu, S., Yu, X., et al. (2013). A role for a dioxygenase in auxin metabolism and reproductive development in rice. *Dev. Cell* 27, 113-122. doi: 10.1016/j.devcel.2013.09.005

SUPPLEMENTARY TABLE S4. Primers used in this study.

A. Cloning		
Primer name	Forward primer (5' to 3')	Reverse primer (5' to 3')
OsMYB7 coding sequence	ATGGGGAGGTGCCGTGCTGCGA	TCATTCATGGGGAGGCTCTGA
osmyb7-1 guide RNA	GGCATGTCAGGTGGTCTCTGATCG	AAACCGATCAGAGACCACCTGACA
B. Genotyping		
Primer name	Forward primer (5' to 3')	Reverse primer (5' to 3')
OsMYB7-OE1 LP/RP	TCTAACATTGAGGTGACCG	GTTACTTGTGCGAGGAGG
OsMYB7-OE1 BP/RP	CGTCGCATGTGTTATTAAAG	GTTACTTGTGCGAGGAGG
35S::OsMYB7	CTATCCTTCGCAAGACCCCTT	ATGCAGAGGTCCAGGTTGA
CAS9	CTGTAGAGTCTGTGTTCAAAT	AACTGAAGGCAGGAAACGACAAT
C. Transactivation / Transrepression activity assay		
Primer name	Forward primer (5' to 3')	Reverse primer (5' to 3')
OsMYB7-pGBK7	GTCGACTCATGGGGAGGTGCCGTGC	GC GCCGCTCATGGGGAGGCT
OsbHLH079-pGBK7	GAACGGGTGAGGAGGGAGAGGATCAG	GC GCCGCTACATTTCCATTTGAGA
rGAL4	CCATGGGAGCCAATTAACTAAAGTG	GAATTCCTCTTTGGGTTGGTGG
OsMYB7-rGAL4	GTCGACTCATGGGGAGGTGCCGTGC	GC GCCGCTCATGGGGAGGCT
ONAC026-rGAL4	GTCGACTCATGGGAGAGCAGCAGCAG	GC GCCGCTCAGTACTCCAGATGGT
D. RT-qPCR		
Primer name	Forward primer (5' to 3')	Reverse primer (5' to 3')
GAPDH qPCR	AAGCCAGCATCTATGATCAGATT	CGTAACCCAGAATACCCCTGAGTTT
OsMYB7 qPCR	CTCGGCAACAAGTGGTCTGTAT	GATCCCCCTGCCGAGAACGTT
OsPAL1 qPCR	CCGCTTCGTATCTCAGAC	CAGCTAACACAAGAACACGAGA
OsPAL2 qPCR	GACGTATAGCAACACAAAACGT	GAAACAGCAACAGTAACATCAAG
OsC4H2 qPCR	GGTAGTTATGTTGTTCTG	TGAACCAACAAGTATAAGAAAAAA
Os4CL3 qPCR	GAGATATGATGTTGCTGTCCA	TTTTATGAACATTGACAAGCTG
OsHCT1 qPCR	CAGGCTGAGCACATGGGAGAA	CTCTAGCTCTACAACCTCCCT
OsHCT2 qPCR	GATTCCACACGTTAGTCCCTGC	CAAATGTGCTCTGCCAAAAGC
OsC3H qPCR	TGCTTGTGAATGAACGAATC	CATCGCTTGTGTTAATCA
OsCOA1 qPCR	CGATGCCCAAGAACTAGTC	ATAACATTCCAGTAGCTTCAA
OsCOA20 qPCR	CTCTCTACTGTCACAACTATAC	GTAGTACAGTAACAACCATCATC
OsCCoAOMT1 qPCR	TAGCCCCAAGACCCCTCTCAA	ATAGGTGTGCTCGCTGGTGT
OsCOMT1 qPCR	CGTGGGTAATCATGTCGTTG	TTAGAACTCAGAATCACCAGAAT
OsCCR17 qPCR	CTGCTGGCTGCTGATATATAC	TGTCGATCGGTGTGATGTAG
OsCCR19 qPCR	AGTGTAGGCATCTGTTGTTA	CACGTCTGTTTATTCAATGAT
OsCCR20 qPCR	GAGCATGAGGAAAACAGCAGA	CTACTTGGTTTACAGCACCG
OsCAD2 qPCR	CTTGAACCTGTTGTTGAGACTC	TGGCCATATATTGCGAGGC
OsCAD6 qPCR	TTAATTATTGGAGGCTGCA	TTCTGAATAAGTACAAAGTGC
OsCESA1 qPCR	TCATGGGCAGGGAGAACCGC	CAGTTCACACCGCATTGCCCA
OsCESA3 qPCR	ATCGGTGTGCTGAAGGAATAC	GAAGTTCACAAAGGTTGCCGCA
OsCESA5 qPCR	GGATGGATCTCCGCTCTGGA	AGGAACAAGGAATGAAACAGCCC
OsCESA6 qPCR	CAGCCTACACTCCATATGCGG	TGGAACAAAAGAAATGCCGGAGAT
OsCESA8 qPCR	TGCCAGTTGTTTCTGAAATAC	TATTCTGGTCTGTACGTAGCTGT
OsCSLA1 qPCR	GCCTTTCTCTGTTATGTCATTGT	CTCCTTGCCCATGACACC
OsCSLA6 qPCR	ATGCTATGACTACTGTACAGAGATGA	AGACACTGACGCCCATGAAAT
OsCSLC1 qPCR	GGGGGTTAACATTATCGGAGA	AAACAAACCCATTCAACCACTGAG
OsCSLC7 qPCR	AAGAGTGTGAAATGTTGATG	ATCTATCTACATCTCACAGTTCA
OsCSLC9 qPCR	ACAGTGACAATGGAGGTGCT	GGGGGTGTACATTGTGGATCAT
OsCSLD2 qPCR	CAAGGGGCTATGGGAAGGAG	GGCAACCCACAGCAATGAGA
OsCSLE1 qPCR	GTGTTTACCCAGGCCATC	TGACTGCTGTTGGTATTCTCC
OsCSLF6 qPCR	CCGGAGACGAAGAAGAAAACACA	GTTGCAGCAGCGTGTAGTAGAA
OsCSLH1 qPCR	AGAACTACTCGCCATGGAAG	ACCGCTCCAATGCTTCACTTT
OsBRD2 qPCR	GAGGCGTAATTCGTTGAGACC	CGATGACAGGATTACAAAGTGC
OsD2 qPCR	GCCACCACTACTATACCGATC	TCGTGTGGCTACTCGTACT
OsD11 qPCR	GGTAGATATTTGTCCATGCCG	AGCAGATGAAAGTTGAAACAGTGG
OsDWARF4 qPCR	GAGCCTTITGACCTAATTGTTGGA	CGAAAACGTGACATGCATCCT
OsBRD1 qPCR	GATGACAGGATTAGAACAGCCG	GATGGACAAAAGAAATACAGGAGC
OsBRI1 qPCR	CTCCTCATCACTCCCCACTCTCC	AGCTCACTGCCTCACGACC
OsBAK1 qPCR	CTCAACTCAACCCCCCCCCAA	GATCCCCTCTCGCTTTCG
OsBSK3 qPCR	CATGCCCTTGACCTGATTGAG	TCGCACTAGTCTGTCCTTCC
OsGSK1 qPCR	CTAAGTGTGGAGACGGGG	AGGCAGATGACATTGGGGTG

OsGSK2 qPCR	AGACCTTTGTTGGATCGTTTCG	TTCTCTTGTGTTGCGGGGATT
OsBZR1 qPCR	GCCGAGCAAAAAGATGGTCC	GAATGAAATCGCCCCAATCGCA
OsLIC qPCR	GTTGCCACCATATGCGTACTT	CACTGTTCACTCTGCAAATTCTCT
OsDLT qPCR	GGCTGTTGAGAGAGACTCCC	ATAGTGACTGTGAGAGATGCTGC
OsRLA1/SMOS1 qPCR	ATCCTGCACGTCATGGGTTTC	ACTTCTCTTACCTCTATTCATGGCT
OsD1/RGA1 qPCR	AAGTCACACAGGGAAAGTAATTAGG	CAAAAGATCAATCAATGGCCACGT
OsTUD1 qPCR	GAGTGGAGTTTGAATTGCTG	GCTGTCGACTGCAATTGCTA
OsBU1 qPCR	GGATGATATGAATGCGACTCGT	ATCATCATCATCAGTAGTACACCG
OsTAA1 qPCR	TTGTAAGTTGAAGTCCTGCCA	AAAACACAACATCGAGAAACAA
OsYUCCA3 qPCR	AGCTAGTAGGTTGGTGGTGATA	CGCACGCAATTACACCCCTT
OsYUCCA4 qPCR	GCTGGTCTGGTTACATTCA	GGGGAAAAAAATGAGATGCAC
OsYUCCA5 qPCR	GTTCTGTCGTCGCTGTGTT	GATTGATCTCATTCTCGACCAGC
OsYUCCA6 qPCR	ACATTGATGAGGAGGCCAGA	CATTCTGTACATAAAGGCCAT
OsYUCCA7 qPCR	ACCGTTGACTGCTACTC	GTATGATCACACTCTCTAGCTT
OsGH3-1 qPCR	GCAATGGAACAAAAGCAAGGA	CAGATCATCACCCCTCTAGCTCAA
OsGH3-3 qPCR	CCTCTTAATGACGATCTGCTCTG	GGATCCGAGCTGCTGATAAGA
OsGH3-4 qPCR	AGAGAGAATTGCTAGTATGGT	CTACCTGAACTAACACTCGTTGATTA
OsGH3-6 qPCR	CACTAGCATCTGCTCATGGTCA	ACCTTGTCACTGCCGGAATT
OsGH3-7 qPCR	ATTGGAGGAAAGGGTTGAGGAA	CTCCTCTAAATTGGCTGAA
OsDAO qPCR	ATGCTGAGGGGATGGGAATT	CTCACACCTCCAGTTATTCTAC
OsCycD4;2 qPCR	GGGGCCAAAAGGGAGGGAAAT	CTTGGGGGCACCTCTCATCA
OsCycD6;1 qPCR	AGGCAACGTGAGCGAGAGATAG	AGAAAGAGCAGGGCAAGAGCAA
OsCycH1;1 qPCR	AGGTGAGGTTCCGTTTAGCC	CACAAGATTACAAGAAGGCGAGG
OsCycU1;1 qPCR	GAGCGCGTCTGTGTATATATC	CACTTGGCAGTAATTAAATCCGTC
OsCycU3;1 qPCR	CAAGTTCACGGCGTCAATAGCA	TACCGCATCAGCTCGCTTT
OsCycU4;1 qPCR	AGCTCTCTTTTGTCACTGGA	AGCTCAATTCTTCACTAACACAA
OsCDKA;2 qPCR	TAAGTTGGTGTGCTCCCTCC	CAGAGGGATAGCCAGGAGGTA
OsCDKB;1 qPCR	GTTAGCAGCAAGGAATTGTT	CCATACAGCATAGAAACAAACCC
OsCDKC;2 qPCR	GCGGTATCATGAGCAGCAAAT	ATACCTCCGAGAGATGCCCTGG
OsCDKD;1 qPCR	CATAGATGAGTTGTTGTGAG	CACCGAAAAGAACCTGAGACATAAAC
OsCDKE;1 qPCR	ATTTGGTGTGTTACTGTGAGC	CAATTCTCACTGTACGACTAGGA
OsCDKF;1 qPCR	ATGGGCTAATTCAAGGGTTGG	AAATTCCCTCTGCCAGCATGTT
OsEXPA1 qPCR	AAGTTGGAGCATGCGCGC	CAAGCACCTCGCAAACGTAC
OsEXPA4 qPCR	TCGTCGTCGTCCTTCTCCCTT	TCAGCGATAGCCAAAACCTCT
OsEXPA6 qPCR	AGTAGATGCTGAGGTTGCTGTG	AACTAAGAGCAGAGCAGCAAAC
OsEXPA10 qPCR	AGAAATGTTAGTGCAGAGC	GTAGTGCATTATCAGAGTTCC
OsEXPB3 qPCR	ATTTGAGATCGATCGTTGGC	CAAAACGAACCTCTGATGACA
OsEXPB4 qPCR	GGGTTCTTGAGTTGTTGGGG	CCTCCCTCATTCCCACACAG
OsEXPB6 qPCR	CTGGTCTAGTGTGTGAAGT	CTGTAGCCTTAAGATTGGTT
OsEXLA2 qPCR	CATGTACAGTTTTTGCTTCCCTT	CTGTGGCTCTTAATTGATGGAT
OsEXLA3 qPCR	GACGTATCTGGCACTGCAAAG	GTTTGACAGGGAAAGGGGAGC
OsXTH9 qPCR	CCCGAGTGTCCATGCCGTA	TGAGTTCGATCGAGTCCGGGTTC
OsXTH10 qPCR	CCCCTGAATCTCCACACAC	GATCAATGGGGGAGCTCGAA
OsXTH11 qPCR	ACACGAGAAGATGATCATAACG	ATTATTGCGCATCTGACGTG
OsXTH12 qPCR	TCTGTATCTATTGCTGTATGTG	CTTATTATACATCCATCGTCGT
OsXTH15 qPCR	CTCTGGTTGTATGCTCCGGAC	CCGATGGACGATGTGTAGTAGG
OsXTH17 qPCR	GATGAGTTCTGGCAATGATT	AAACAAATGGAGAACGAATGGA
OsXTH21 qPCR	CCCGAATGCTGAGCTACTTT	ACACAACACACAGCAATCAGC
OsXTH23 qPCR	TTGGGAAGCTAATGGCATATG	GCACCTACTACCTTACAAAC
OsXTH28 qPCR	ATTCCCGCGCTCTGACCGAT	CCAGGAAACTATAATCACGTACGAC